

Frequency Modulation based Resistive Sensing for Wearable Galvanic Skin Response

Md Shamsul Arefin
Biomedical Integrated Circuits
and Sensors Laboratory
ECSE Department
Monash University,
Melbourne, Australia.
md.arefin@monash.edu

Jean-Michel Redouté
Biomedical Integrated Circuits
and Sensors Laboratory
ECSE Department
Monash University,
Melbourne, Australia.
jean-
michel.redoute@monash.edu

Mehmet Rasit Yuce^{*}
Biomedical Integrated Circuits
and Sensors Laboratory
ECSE Department
Monash University,
Melbourne, Australia.
mehmet.yuce@monash.edu

ABSTRACT

This paper presents a frequency modulation based readout circuit for the measurement of skin conductance or resistance. A charge pump based frequency-to-voltage converter circuit with adjustable sensitivity is used to convert the frequency shifts due to skin resistance changes into voltage variations. The readout circuit improves the measurement accuracy and artifact rejection in measurements of the galvanic skin response on the skin, and can be integrated with wearable physiological monitoring systems. The readout circuit is designed and fabricated using the UMC 0.18 μm CMOS technology. It occupies an area of 0.18 mm^2 and consumes 11.7 mW.

Keywords

Galvanic skin response, Frequency modulation, Frequency-to-voltage converter

1. INTRODUCTION

For monitoring health, activity, mobility, and bio-potential continuously, extensive research has been performed in the field of wearable biosensors and physiological monitoring systems [1, 2, 3, 4, 5]. The major vital signs are electrocardiogram (ECG) for electrical activity of cardiac, heart sounds, electromyogram (EMG) for electrical activity of a muscle, electroencephalogram (EEG) for electrical activity of brain, electrical conductivity of skin, blood glucose, respiration rate, mobility for limb movement, and skin temperature [2, 4]. The sensors and low-power readout circuits with wireless are integrated to develop wearable physiological monitoring systems.

^{*}Mehmet R. Yuce's work was supported by Australian Research Council Future Fellowships Grant FT130100430.

The galvanic skin response (GSR) is an indicator of sympathetic and parasympathetic nervous system activity that affect the skin conductivity due to the activity of sweat glands [4, 5]. Since the sweating is controlled by sympathetic and parasympathetic nervous system, skin conductance is a means for the measurement of sympathetic and emotional responses [6, 7, 8, 9]. The sympathetic response due to excitations increases sweat in sweat glands that results in parallel low-resistive pathways. As a result, the conductivity of the skin increases. The parasympathetic response due to relaxation diminishes the low-resistive pathways, and therefore, decreases the conductivity of the skin. The electrodes are positioned on the fingers and/or palm.

A readout circuit is needed to convert the skin conductance or resistance to measurable voltage levels. To measure the skin resistance, a constant current is applied across the electrodes, or a constant voltage is applied across a known resistor and the electrodes in series [1]. Amplifier based readout circuit is also utilized to measure skin resistance. These circuits provide amplified voltage change proportional to the skin resistance change [5]. Various noise sources such as flicker noise ($1/f$ noise), thermal noise, amplifier noise, and substrate-noise coupling minimize the sensor readout range and resolution of these circuits [10].

In this paper, a frequency modulation based readout circuit is used for detecting galvanic skin resistance. A frequency-to-voltage converter (FVC) is used to convert the frequency shifts due to skin resistance into voltage change with adjustable sensitivity [11]. The feedback control system minimizes the overall power consumption and presents a low power alternative for resistive readout circuits. This circuit can be integrated with wearable physiological monitoring systems. The readout circuit for galvanic skin resistance is presented in Section II. The experimental results are discussed in Section III. Section IV presents a summary of this paper.

2. INTERFACE CIRCUIT

The block diagram of the readout system for skin resistance is shown in Fig. 1. A differential crossed-coupled VCO is implemented to convert skin resistance changes (ΔR_{sen}) into frequency variation (ΔF_{vco}). A sine-to-square (STS) converter circuit converts ΔF_{vco} from the VCO into time-

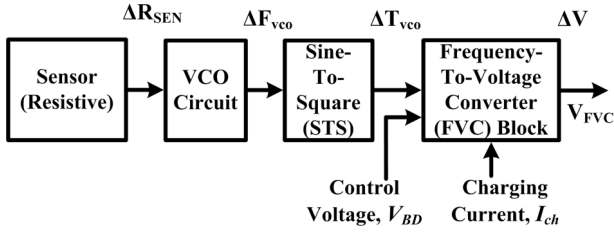


Figure 1: Block diagram of the proposed resistive sensor interface system.

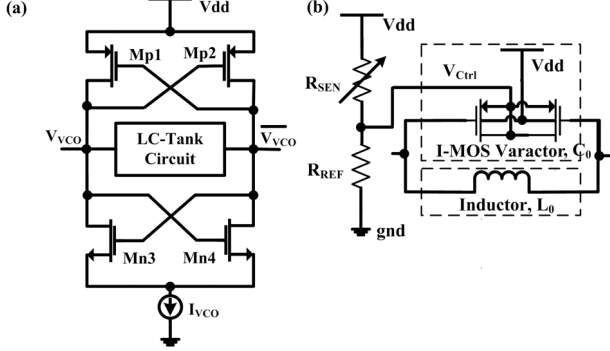


Figure 2: (a) Schematic of crossed coupled differential VCO circuit with a configurable LC-tank circuit. (b) The schematic of the LC-tank circuit for the resistive sensor system where sensor (R_{SEN}) is in series with a reference resistor (R_{REF}) to produce a varying control voltage (V_{ctrl}) with respect to R_{SEN} .

period variation (ΔT_{vco}). A frequency-to-voltage converter (FVC) circuit is designed to convert ΔT_{vco} as the voltage changes (ΔV) [11].

The schematic of a differential crossed coupled VCO employing an inversion-mode MOS (I-MOS) varactor is illustrated in Fig. 2(a). The I-MOS varactor, C_0 [12] and inductor, L_0 act as the LC-tank of the VCO (Fig. 2(b)). The C_0 is dependent on the source-drain voltage, V_{ctrl} . The effective capacitance is modeled by $C_0(V_{ctrl}) = C_{min} + C_V(V_{ctrl})$ for $V_{ctrl} > 0$ condition [12]. Here, C_{min} is the minimum fixed capacitance of the varactor and C_V is the additive capacitance component that depends on V_{ctrl} . The skin resistance (R_{SEN}) is in series with a reference resistor (R_{REF}) to produce a varying control voltage (V_{ctrl}) with respect to R_{SEN} . The varying voltage, V_{ctrl} , resulting from skin resistance is translated to frequency variation using the VCO. The VCO oscillation frequency can be approximated for this configuration as $F_{vco} = 1/2\pi\sqrt{L_0(C_{min} + C_V(V_{ctrl}))}$. The time period of the oscillator for V_{ctrl} can be expressed as $T_{vco} = T_0(1 + C_V(V_{ctrl})/2C_{min})$. Therefore, the change in time period is

$$\Delta T_{vco} = \frac{\Delta C_V(V_{ctrl})}{2F_0 C_{min}}. \quad (1)$$

The FVC block comprising of the logic controller block and a charge pump (CP) circuit, is illustrated in Fig. 3(a). An external control voltage (V_{BD}) and a feedback voltage (V_{FVC}) from the CP circuit provide the control to translate the

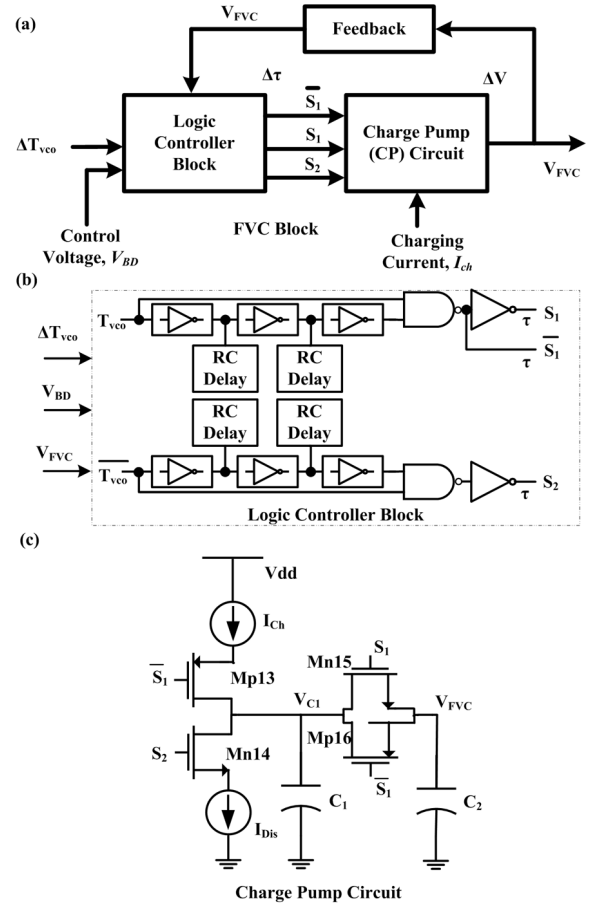


Figure 3: (a) Block diagram of the FVC circuit with feedback charge pump. (b) Schematic of logic controller circuit. (c) Schematic of the charge pump circuit.

ΔT_{vco} into pulse-width variations ($\Delta\tau$). Figure 3(b) shows the logic controller block that produces three control pulses (S_1 , \bar{S}_1 , and S_2) to control the CP circuit in response to F_{vco} , external control voltage (V_{BD}), and a feedback of FVC output voltage (V_{FVC}). Figure 3(c) shows the charge pump circuit. It is composed of two capacitors C_1 and C_2 , transistors ($Mp13$, $Mn14$, $Mn15$, and $Mp16$) acting as switches, and two current sources I_{ch} and I_{dis} . The description and operations of the FVC block are explained in [11].

The FVC output voltage for the varactor capacitance and time-delay feedback can be approximated as

$$V_{FVC} = \frac{1}{(1+P_c K_{FD})} [Q_c \Delta C_V(V_{ctrl}) - P_c K_{BD} V_{BD} + 2C_{min} Q_c - T_{ID} P_c + 1]. \quad (2)$$

where $Q_c = P_c T_0 / 2C_{min}$, $P_c = I_{ch} / C_1 - 1 / R_2 C_2$, and T_{ID} is the fixed delay from inverter. Here, K_{FD} and K_{BD} are the slopes of RC delay circuits. From (2), the slope of the V_{FVC} for the variation of $\Delta C_V(V_{ctrl})$ is $Q_c / (1 + P_c K_{FD})$. Since, P_c and Q_c are proportional to I_{ch} , the slope of V_{FVC} is controlled by I_{ch} . The VCO and FVC circuits are fabricated in the UMC 0.18 μm CMOS process and occupy an active area of 0.18 mm^2 .

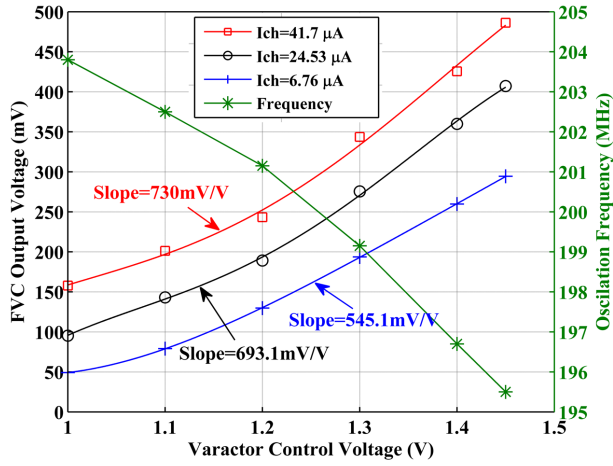


Figure 4: Experimental measurement of FVC output voltage and VCO oscillation frequency for the variation of varactor control voltage.

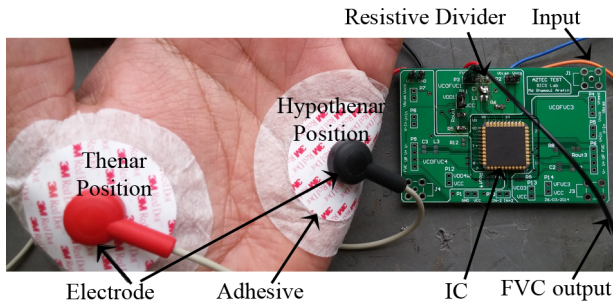


Figure 5: Experimental setup for the GSR measurement.

3. EXPERIMENTAL RESULTS

The performance of the FVC circuit is verified by applying a set of controlling parameters (I_{ch} and V_{BD}) for the variation of off-chip (SMD) resistors. Then, the readout circuit with FVC is evaluated for the measurement of GSR under the influence of controlling parameters.

The experimental measurements of the FVC output voltage for the variation of V_{ctrl} is shown in Fig. 4. The VCO circuit ($L_0=15$ nH) modulates from 203.8 to 195.5 MHz for the variation of V_{ctrl} from 1.0 to 1.45 V. The V_{ctrl} that changes according to the SMD resistors, is converted to frequency variations with a sensitivity of 18.44 MHz/V. The FVC translates the frequency variations to voltage variations with a sensitivity of 693.1 mV/V for I_{ch} of 24.53 μ A. If I_{ch} is increased to 41.7 μ A, the sensitivity increases to 730 mV/V, whereas the sensitivity decreases to 545.1 mV/V for a decreased I_{ch} of 6.76 μ A. The V_{BD} is fixed at 0.4 V. As a result, the sensitivity of the output voltage is also controlled by the I_{ch} .

The GSR is measured by using two dry Ag-AgCl electrodes placed at the thenar and hypothenar positions of the palm, as shown in Fig. 5. The area of the each electrode is 1 cm². The range of galvanic skin resistance is 0 to 100 K Ω . The readout circuit is connected to measure skin resistance, as

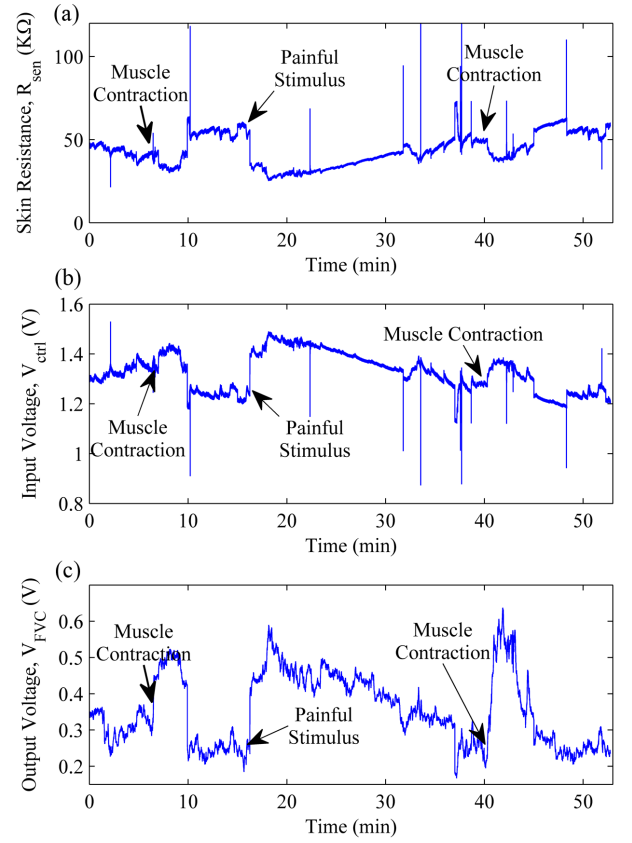


Figure 6: Time-domain plot for muscle and painful stimulus of (a) the skin resistance, (b) input control voltage from resistor divider circuit, and (c) FVC output voltage.

shown in Fig. 2(b). The reference resistor, R_{REF} is 121 K Ω and the supply voltage, V_{dd} is 1.8 V. The LC-tank of the VCO circuit is set by L_0 of 15 nH to convert the resistance changes to frequency shifts. The I_{ch} of 41.7 μ A and V_{BD} of 0.7 V is used to convert the frequency shifts to voltage change.

The time-domain plot of the resistance (R_{SEN}) from GSR response, input control voltage (V_{ctrl}) from resistor divider circuit, and FVC output voltage (V_{FVC}) for muscle and painful stimulus are shown in Fig. 6. The acquired signals are sampled at 1000 samples/s and digitized at 12-bit resolution. The muscle contractions are performed at 6th and 39th minute of the experiment. The muscle relaxations are performed after 1 min of muscle contractions. The painful stimulus of pinprick is performed at 16th minute of the experiment. The muscle contraction and painful stimulus increases sweat secretion that in turn decreases the resistance and increases the input control voltage. The reverse events decreases the input control voltage. The input control voltage from GSR response produces noises due to the artifacts caused by motion, skin-electrode contact, and sweating. The FVC output voltage, which provides lower noises and higher temporal correlation, improves the detection of high-amplitude events compared to the simple resistor divider circuit. It also provides higher sensitivity to smaller

Table 1: Comparison of the interface circuits for GSR measurements.

Circuit Method	Implement	Sensors	Sensor Position	Applications	Ref. (Year)
Amplifier	Discrete	Ag-AgCl Electrodes	Thenar-Hypothenar (Palm)	Physiological Monitoring	[5] (2008)
Amplifier with LPF	Discrete	Ag-AgCl Electrodes	Finger	Emotion Recognition	[6] (2004)
NA	Commercial	Electrode (S220)	Finger	Driver's Emotional State	[7] (2011)
NA	Commercial	Stainless Steel	Arm	Soldier Stress Monitoring	[8] (2007)
Frequency Modulation	IC	Ag-AgCl Electrodes	Thenar-Hypothenar (Palm)	Physiological Monitoring	This Work

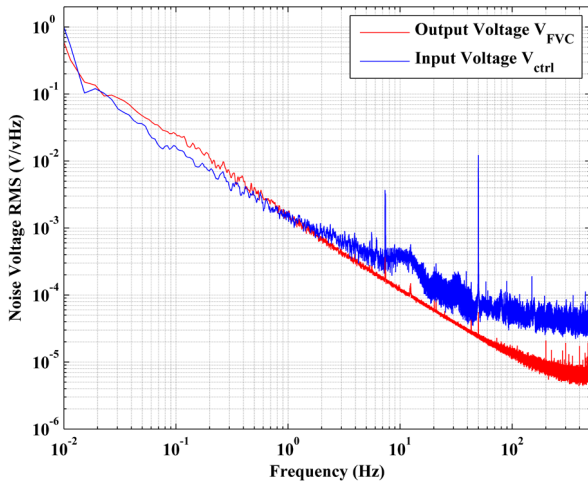


Figure 7: Measured spectral density of the FVC output voltage and the input control voltage.

amplitude events that were ignored in standard GSR recording.

Figure 7 depicts the measured spectral density of the FVC output voltage (V_{FVC}) and the input control voltage (V_{ctrl}) of the readout circuit. The signals were recorded for each 40 minutes. The $1/f$ corner frequency at the output of the circuit is 100 Hz, which is lower (around 500 Hz) than the input of the circuit. The measured thermal noise floor is $47.84 \mu V/\sqrt{Hz}$ at the input of the readout circuit. A decrease in the thermal noise floor of $8.14 \mu V/\sqrt{Hz}$ is observed at the output of the readout circuit. Table 1 show a comparison for the GSR measurement techniques with previous techniques in the literature.

4. CONCLUSIONS

A low noise, low power, and high resolution galvanic skin resistance readout circuit is presented. The circuit is designed using the UMC 0.18 μm technology. The changes of resistance are translated into VCO oscillation frequencies and pulse-width of control signals, which are detected using the FVC circuit as voltage outputs. The circuit has been evaluated for the events of muscle and painful stimulus. This circuit provides improved measurement accuracy and artifact rejection in measurements, higher sensitivity, and lower noise level compared to the resistor divider circuit.

5. REFERENCES

- [1] U. Anliker, J. A. Ward, P. Lukowicz, G. Troster, F. Dolveck, M. Baer, et al. AMON: a wearable multiparameter medical monitoring and alert system. *IEEE Trans. Information Technology in Biomedicine*, 8:415-427, Dec. 2004.
- [2] M. Chan, D. Estéve, J.-Y. Fourniols, C. Escriba, and E. Campo. Smart wearable systems: Current status and future challenges. *Artificial intelligence in medicine*, 56:137-156, Nov. 2012.
- [3] M.R. Yuce. Implementation of wireless body area networks for healthcare systems. *Sensors and Actuators A: Physical*, 162(1):116-129, Jul. 2010.
- [4] T. Vuorela, V.-P. Seppa, J. Vanhala, and J. Hyttinen. Design and implementation of a portable long-term physiological signal recorder. *IEEE Trans. on Information Technology in Biomedicine*, 14:718-725, May 2010.
- [5] P. Pandian, K. Mohanavelu, K. Safeer, T. Kotresh, D. Shakunthala, P. Gopal, et al. Smart Vest: Wearable multi-parameter remote physiological monitoring system. *Medical engineering & physics*, 30:466-477, May 2008.
- [6] K.H. Kim, S.W. Bang, and S.R. Kim. Emotion recognition system using short-term monitoring of physiological signals. *Medical and Biological Engineering and Computing*, 42(3):419-427, 2004.
- [7] C.D. Katsis, Y. Goletsis, G. Rigas, and D.I. Fotiadis. A wearable system for the affective monitoring of car racing drivers during simulated conditions. *Transportation research part C: emerging technologies*, 19(3):541-551, 2011.
- [8] C.H. Perala and B.S. Sterling. Galvanic skin response as a measure of soldier stress. (No. ARL-TR-4114). *Army research lab*, May 2007.
- [9] W. Boucsein. Physiology of the Electrodermal System. in *Electrodermal Activity*, 2nd ed. Springer US, 2012.
- [10] N. Yazdi, H. Kulah, and K. Najafi. Precision readout circuits for capacitive microaccelerometers. *Proc. IEEE Sensors 2004*, pages 28-31, Vienna, Austria, 24-27 Oct. 2004.
- [11] M.S. Arefin, J.-M. Redoute, M.R. Yuce. A MEMS Interface IC With Low-Power and Wide-Range Frequency-to-Voltage Converter for Biomedical Applications. *IEEE Trans. on Biomedical Circuits and Systems*, Jun. 2015.
- [12] P. Andreani and S. Mattisson. On the use of MOS varactors in RF VCO's. *IEEE J. Solid-State Circuits*, 35(6):905-910, Jun. 2000.